Expanded View Figures

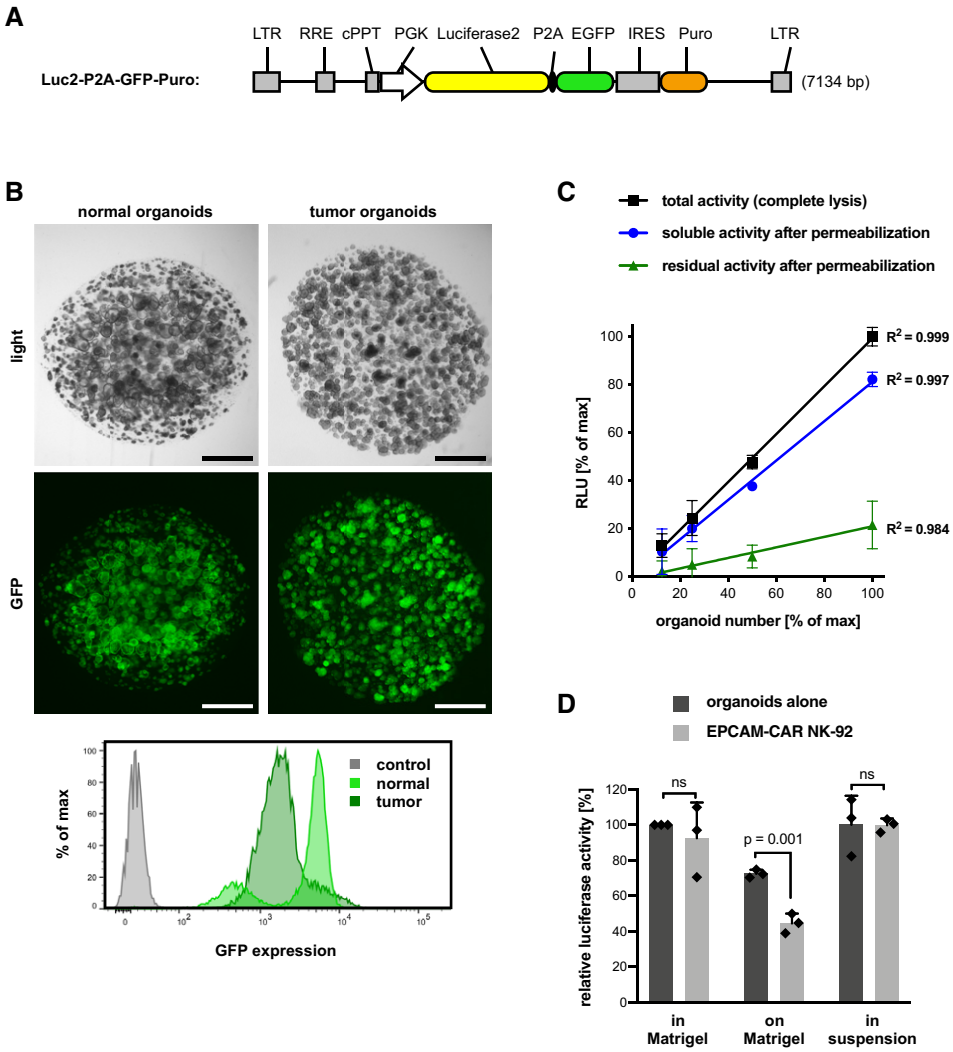

Figure EV1. Luciferase activity as a quantitative read-out for lysis-resistant target cells.

A Lentiviral construct to drive co-expression of luciferase 2 and EGFP (separated by a P2A peptide). Stable expression is selectable by the puromycin resistance marker. Additional features are long-terminal repeats (LTR), Rev response element (RRE), cPPT central polypurine tract, and the phosphoglycerate kinase (PGK) promoter.

B Patient-derived normal and tumor colon organoids were lentivirally transduced to stably co-express luciferase and GFP. Homogenous expression of GFP was observed. Scale bars: 1,000 μm. Bottom: Flow cytometric analysis of GFP expression. GFP-negative organoids are shown as control.

C Linear detection of viable organoids. Luciferase activity (in relative light units, RLU) was quantified either after complete lysis (black line), or in the supernatant (blue line) or the remaining cell debris (green line) following cell permeabilization. Mean values (± SD) from $n = 3$ replicates. The coefficients of determination (R^2) are displayed. An organoid number of 100% corresponds to 1.25×10^5 epithelial cells. Note that residual signal after lysis was below 20% of total activity.

D Quantification of luciferase activity in different co-culture settings (as in Fig 1G). Mean luciferase activity (± SD) from $n = 3$ replicates relative to growth in Matrigel. The presence of EPCAM-CAR NK-92 cells (E:T ratio was 1:1, for 8 h) reduces luciferase signal of normal organoids after seeding on a Matrigel-coated surface. No reduction is detected after organoid seeding in Matrigel or in suspension. The experiment was repeated three times. Significance was analyzed by unpaired *t*-test. Note that organoids were seeded on Matrigel 24 h before the start of co-culture, which causes reduction of signal compared to standard culture.

Figure EV2. Imaging-based quantification and tracking of individual organoids.

A Kinetic imaging data of single organoids (see Fig 3B and C). GFP-positive organoids cultured alone or with parental NK-92 cells or EPCAM-CAR cells. NK-92 cells were labeled with anti-CD45-APC. Maximum intensity projections of merged channels and the single GFP channel are shown. Organoid areas detected by the analysis software and expanded areas for determining NK-cell recruitment are marked in color. Scale bars: 100 μm.

B Linear detection of organoid area. Organoids were seeded on Matrigel layer at different concentrations and co-cultured with parental NK-92 cells or EPCAM-CAR cells. For each concentration, the organoid area was automatically quantified in 110 imaging fields before (0 h) or after (8 h) addition of NK-92 cells. The entire imaging region was subdivided into $n = 4$ quadrants, and the relative organoid area is shown as mean (± SD). E:T ratio was kept constant at 4:1. 50% seeding density corresponds to the standard density. Coefficients of determination (R^2) are shown.

C Workflow for extracting single organoid data. Refer to methods for further details.

D Range correction for tracking of organoids that may grow or move during the analysis. The coordinates of each organoid at $t = 0$ were expanded.

E Single organoid tracking in co-culture with EPCAM-CAR cells (data from Fig 3). Normal organoids were classified as large (area > 6,000 μm^2; $n = 7$), medium (area 2,000–6,000 μm^2; $n = 8$), or small (area < 2,000 μm^2; $n = 8$). The lower detection cut-off was set at 500 μm^2.

F Rate of relative area loss for single organoids of distinct sizes (analysis of data shown in E). Average rate (± SD; measured in $n = 7$–8 independent organoids) is shown. Statistical significance was analyzed by unpaired t-test (ns: $P > 0.05$).

© 2019 The Authors

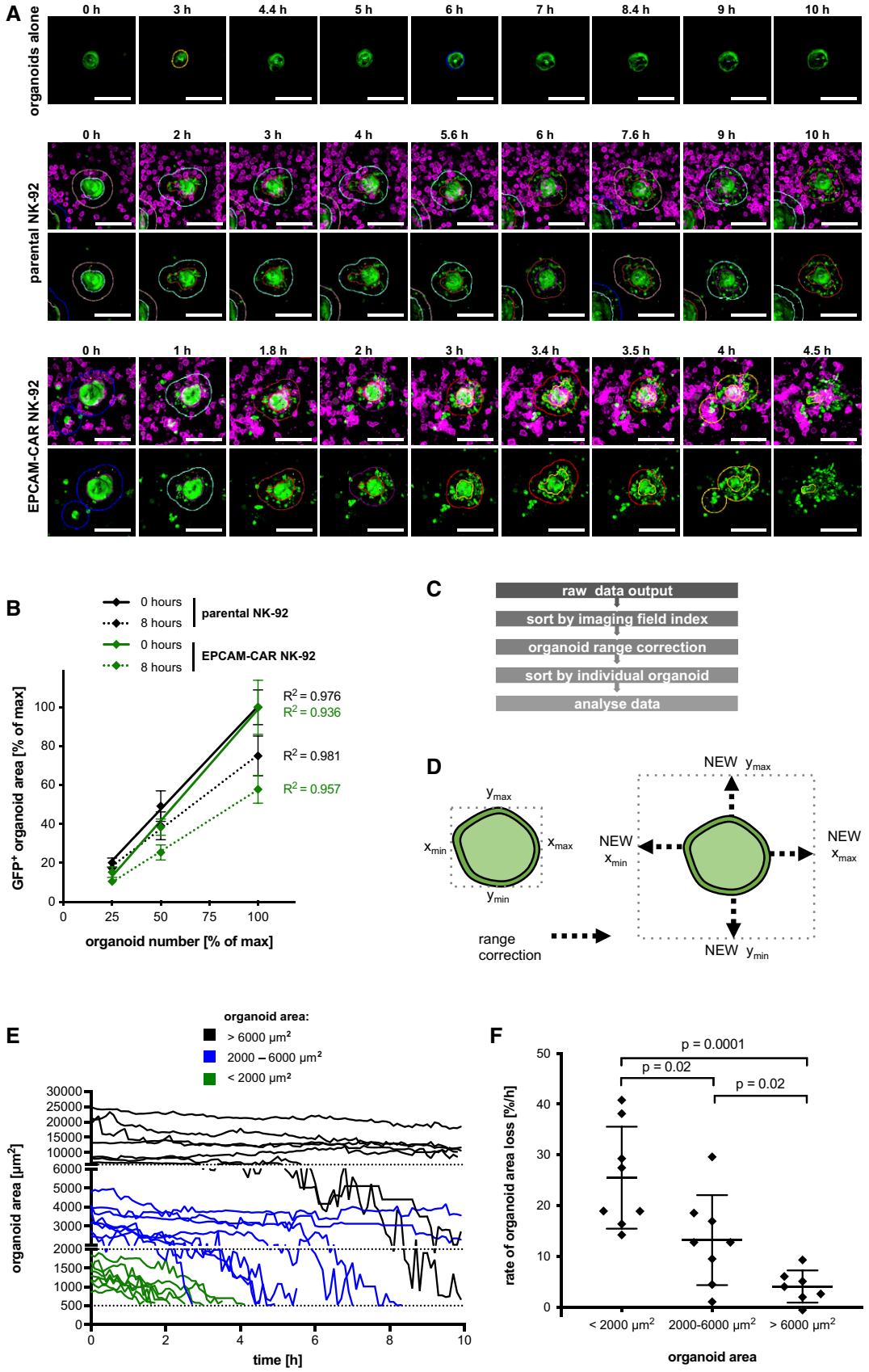

Figure EV2.

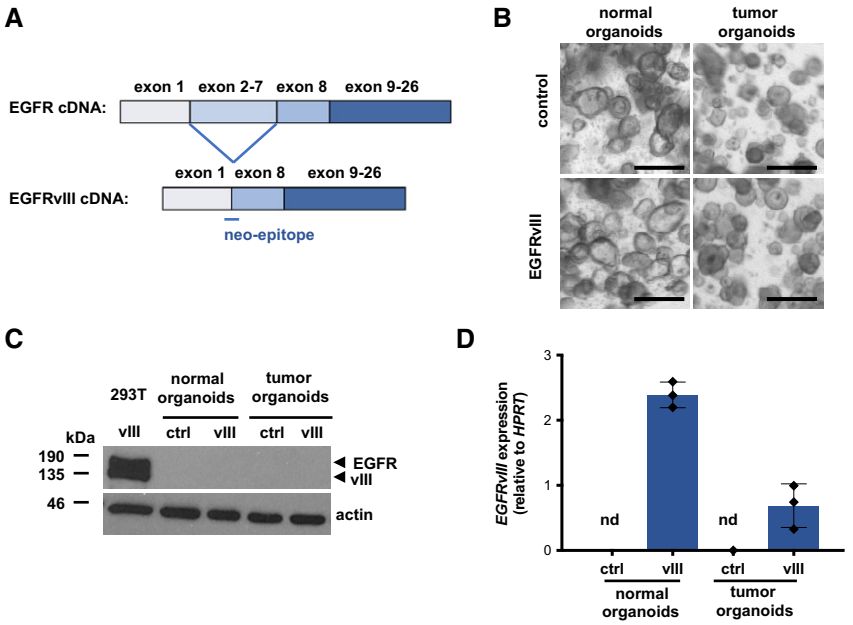

Figure EV3. Generation and characterization of EGFRvIII neoantigen expressing organoids.

A Schematic representations of wild-type EGFR and EGFRvIII cDNA lacking exons 2–7.

B Morphology of control and EGFRvIII-expressing normal and tumor organoids. Scale bars: 250 μm.

C Immunoblot analysis of organoid total cell lysates with anti-EGFR antibody. Actin served as loading control. Lysate of HEK-293T cells transiently transfected with EGFRvIII lentiviral transfer vector served as positive control.

D qRT–PCR analysis of EGFRvIII expression (DNase I-treated organoid total RNA). Average transgene expression (± SD) from $n = 3$ independent experiments (each measured in triplicates) is shown relative to *HPRT* expression level. nd: no expression detected in control organoids.

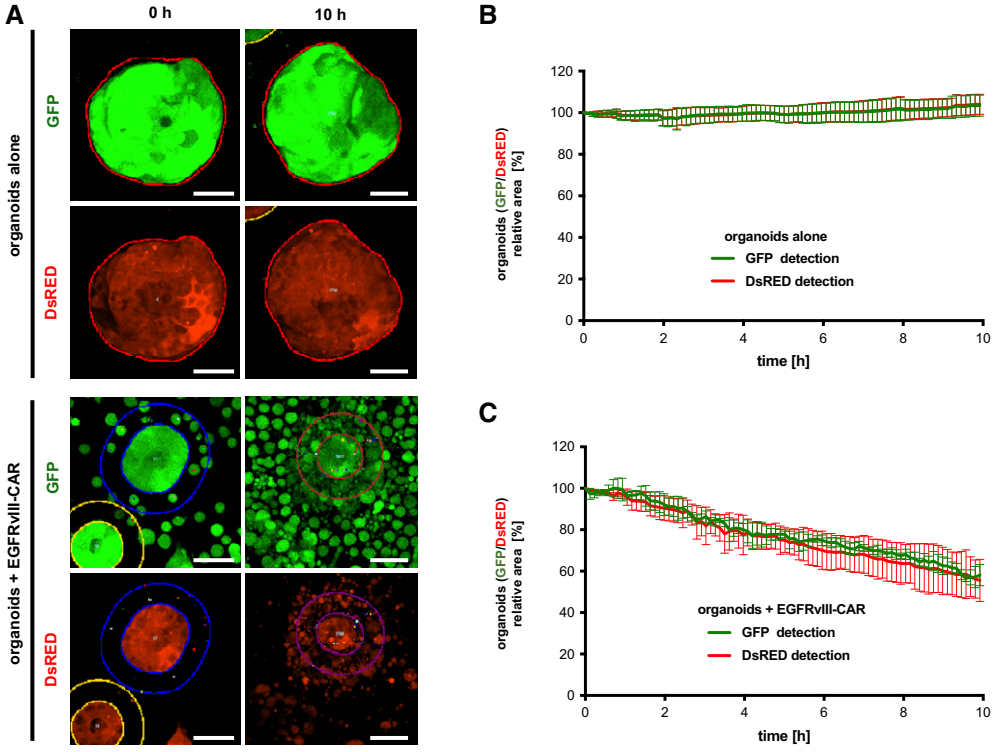

Figure EV4. Image-based detection of organoid cytotoxicity with different fluorescent reporters.

A Imaging data of GFP$^+$ and DsRED$^+$ organoids at 0 and 10 h of monoculture or co-culture with GFP$^+$ EGFRvIII-CAR NK-92 cells (E:T ratio was 2:1). EGFRvIII-positive tumor organoids were used. Maximum intensity projection images are shown. Automatic organoid detection (thin lines) was performed with similar settings for both reporters (see Appendix Fig S2; the outer lines denote the dilated area for analysis of cell recruitment). Scale bars: 50 μm.

B, C Quantitative monitoring of organoid area during monoculture (B) or co-culture with GFP$^+$ EGFRvIII-CAR NK-92 cells (C). Experiments were performed as in (A). Mean values from $n = 4$ imaging positions (± SD) are shown relative to the area detected at $t = 0$. Note that comparable areas are measured for GFP and DsRED channels and that the presence of GFP$^+$ EGFRvIII-CAR NK-92 only minimally affects the detected organoid area.

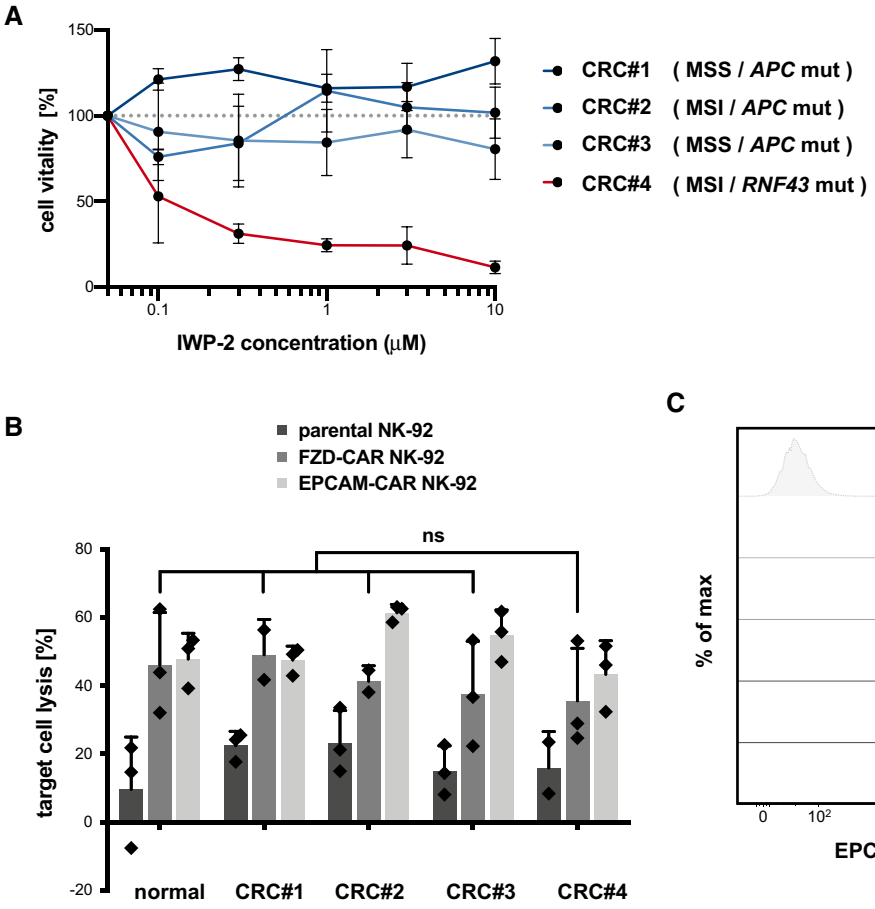

Figure EV5. Evaluation of FZD-CAR NK-92 cells for targeting of human *RNF43*-deficient CRC organoids.

A IWP-2 toxicity assay in different human CRC organoid lines. Cells were seeded in complete medium (– Wnt). Mean cell viability (± SD; in n = 3 wells; CellTiter-Glo assay) after 6 days compared to culture in regular medium. The experiment was repeated twice independently. *RNF43* and *APC* genomic loci were analyzed by Sanger sequencing (see Appendix Fig S4). The status of microsatellite instability/stability (MSI/MSS) and the presence of mutations are noted. *RNF43* mutant organoids (CRC#4) show increased IWP-2 sensitivity, indicating endogenous Wnt-FZD signaling. WT organoids are dependent on exogenous Wnt and were not tested in this assay.

B Luciferase-based quantification of cytotoxicity of parental, FZD-CAR, and EPCAM-CAR NK-92 cells against normal and CRC organoid lines. Experiments were performed in the absence of R-spondin. Mean target cell lysis (± SD; in n = 3 wells) after 8 h of co-culture is shown. The E:T ratio was 2:1. Statistical significance was analyzed by unpaired t-test (ns: $P > 0.05$). Note that the *RNF43*-deficient organoids (CRC#4) show no increased sensitivity toward FZD-CAR NK-92 cells. The experiment was replicated three times independently.

C Flow cytometric analysis with anti-EPCAM antibody shows similar EPCAM surface level on normal and CRC organoid lines. Unstained cells are shown as controls.